LIMNOLOGY
and
OCEANOGRAPHY

ASLO

Limnol. Oceanogr. 9999, 2019, 1–11

doi: 10.1002/lno.11176

Alleviation of hypoxia by biologically generated mixing in a stratified water column

Isabel A. Houghton,[1] John O. Dabiri[1,2]*

[1]Bob and Norma Street Environmental Fluid Mechanics Laboratory, Civil and Environmental Engineering, Stanford University, Stanford, California

[2]Mechanical Engineering, Stanford University, Stanford, California

Abstract

Daily vertical migrations of zooplankton have been shown to affect nutrient distributions and dissolved gas concentrations in lakes and oceans via active internal transport and metabolic consumption. Additionally, mixing generated by these migrations has been shown to have the capacity to alter the physical structure of a water column, with potential further implications for its biogeochemical structure. In this work, we use laboratory experiments to investigate the importance of biologically generated mixing relative to other processes in determining the biogeochemical structure of a water column inhabited by migrating zooplankton. Specifically, we consider oxygen, a highly ecologically relevant scalar, and the competition between metabolic consumption and biogenic mixing in a stably stratified water column with a hypoxic layer. Using laboratory experiments and a one-dimensional model informed by those measurements, we illustrate the potential for migrating animals to alleviate hypoxia, introducing complex feedbacks between the presence of animals and the biogeochemical state of their surroundings. Furthermore, we demonstrate the feasibility of oxygen as a potential indicator of biogenic mixing for future in situ investigations given its low diffusivity and higher signal-to-noise ratio.

Daily vertical migrations of zooplankton are found throughout lakes and oceans, with centimeter-scale animals traversing tens of meters in lakes and hundreds of meters in the open ocean (Ringelberg 2014), often in large aggregations. These movements, the world's largest migration of biomass, are possibly motivated by predator avoidance, allowing feeding at the surface during the night and a return to depth during the day to reduce the risk of visual predation (Ringelberg 2009; Sato et al. 2013). The depth of migration is controlled by a variety of factors, with animals often seeking cover from predation below the euphotic zone as well as within difficult to inhabit regions, such as oxygen-limited waters (Hembre and Megard 2003; Vanderploeg et al. 2009; Bianchi et al. 2013). Because many zooplankton are better able to withstand periods of hypoxia relative to their larger predators, oxygen-limited waters can serve as a daytime refuge (Vanderploeg et al. 2009), and observations of daytime zooplankton location show correlation with oxygen-depleted regions in both lakes (Hembre and Megard 2003) and oceans (Bianchi et al. 2013). Specifically, for an oxygen-stratified lake, zooplankton concentration was significantly enhanced in the "refuge zone" containing 94–156 μmol O_2 L^{-1}, an intermediate level of oxygen where the zooplankton were not physiologically stressed by the reduced oxygen but their larger predators (i.e., trout) could not survive.

By feeding at the surface and subsequently returning to depth when satiated, migrating zooplankton contribute significantly to the active vertical flux of organic matter (Longhurst and Glen Harrison 1988; Zhang and Dam 1997; Manno et al. 2015; Butterfield 2018). Additionally, the active selection of oxygen-limited regions by vertical migrators can intensify the oxygen minimum zones that are simultaneously driving the depth of migration (Bianchi et al. 2013; Butterfield 2018).

Beyond internal carbon transport and metabolic consumption of oxygen, physical mixing generated by animal propulsion has been hypothesized as potentially relevant to the physical structure (e.g., density stratification) of the water column (Huntley and Zhou 2004; Dewar et al. 2006; Katija and Dabiri 2009; Noss and Lorke 2014; Wilhelmus and Dabiri 2014; Wang and Ardekani 2015; Simoncelli et al. 2018). However, non-negligible physical mixing of a density stratification necessitates fluid motion at scales comparable to the length scales of stratification (Osborn 1980), often orders of magnitude larger than an individual zooplankton (Visser 2007). Despite small individual animal size, the behavioral tendency of many zooplankton species to form large, dense aggregations

*Correspondence: jodabiri@stanford.edu

introduces a potentially relevant larger length scale for enhanced physical mixing to occur. A wide variety of field observations report zooplankton aggregations spanning up to tens of meters in the vertical and hundreds of meters in the horizontal (Hamner et al. 1983; Sato et al. 2013). Animal number densities within aggregations have been reported up to 500,000 animals m^{-3} (O'Brien 1988) in the ocean and 1,000,000 animals m^{-3} in lakes (Hembre and Megard 2003) with corresponding animal lengths of 21 and 1.6 mm, respectively. Measurements are typically unique to the location and species and can also be underestimated due to spatial heterogeneity within swarms (Omori and Hamner 1982), but the wide variety of observations in both lakes and oceans indicate the presence of dense zooplankton aggregations in many environments.

Previous laboratory work by Houghton et al. (2018) demonstrated that mixing of a stratified water column is enhanced three orders of magnitude above molecular diffusion by centimeter-scale zooplankton in aggregations with number densities from 46,000 to 138,000 animals m^{-3}. Experiments illustrated the development of large-scale flow, orders of magnitude larger than the individual organisms that transported fluid of different densities against stabilizing gradients. These experiments also indicated significant, irreversible impacts to the density stratification, which in turn can affect the biogeochemical structure by similarly mixing other scalars present, such as dissolved gases or nutrients.

The cascading biogeochemical effects of biogenic mixing are potentially particularly relevant to oxygen depleted zones, which are found in many lake and ocean environments with increasing frequency due to anthropogenic inputs, such as fertilizer runoff. These so-called "dead zones" come with significant ecological consequences due to the general uninhabitability for many organisms (Diaz 2001; Diaz and Rosenberg 2008). In hypoxia-prone waters, migrating zooplankton have the potential to affect the distribution of oxygen, which in turn may drive unique feedbacks on local ecology. In this work, we investigate two competing processes governing oxygen concentrations in the presence of migrating zooplankton, namely oxygen consumption due to the metabolic activity of the animals and vertical redistribution of oxygen due to fluid mixing during animal migrations. To assess the importance of biologically generated mixing in determining the biogeochemistry of a water column, laboratory studies were conducted. In the following section, methods used to achieve controllable vertical migrations of zooplankton swarms in an oxygen and salt stratified tank are described. Direct measurements of oxygen consumption by zooplankton and mixing of an oxygenated surface layer with a hypoxic bottom layer are then reported. A one-dimensional model informed by experimental measurements is used to predict longer term dynamics. An estimate of the dependency of mixing on animal number density is predicted from fluid transport measurements at variable number densities. We conclude with a discussion of the potential broader implications of these results.

Materials and methods

Three different experiments were conducted, one to quantify the oxygen consumption rate in a well-mixed tank, one to assess mixing of a two-layer stratification with a lower hypoxic layer, and one to quantify the dependency of fluid transport on animal number density. All experiments were conducted in a 0.5 m × 0.5 m × 1.2 m-tall clear acrylic tank.

Experimental organism

Experiments were conducted with the brine shrimp *Artemia salina*, chosen for their representative size, 0.5–1.0 cm in length, and swimming mode similar to a variety of marine and freshwater zooplankton (Wilhelmus and Dabiri 2014). Approximately, 125,000 ± 5000 twenty-day-old brine shrimp were obtained from an aquarium supplier (Mariculture Tech) 1 d prior to the experiment and held in 2-liter, aerated beakers of 28 ppt saltwater. Animal age was chosen to optimize between swimming ability and phototactic behavior to allow for the controllable vertical migrations described below. Prior to commencing each experiment, one third of the available brine shrimp (approximately 42,000 ± 1700 animals) were strained through a fine mesh and introduced to the top of the experimental tank, resulting in a tank-averaged animal number density of 140,000 animals m^{-3}.

Oxygen consumption rate

The consumption rate of dissolved oxygen by the brine shrimp was measured over a 48 h period to provide baseline data on their metabolism. The tank was filled with well-mixed saltwater at 28 ppt, oxygenated to 225 ± 1 μmol L^{-1}, and the top of the tank was covered with plastic film to limit oxygen exchange with the atmosphere. Approximately 42,000 ± 1700 twenty-day-old animals were introduced to the tank and left to swim freely with the tank in darkness over the course of the control experiment. An oxygen optode (Unisense) continuously submerged in the tank measured oxygen levels with an accuracy of 1 μmol L^{-1}.

Density-stratified hypoxic water column

A hypoxic water column was created utilizing the animals to consume the oxygen prior to migration experiments. Twenty-five-day-old brine shrimp were left in the covered experimental tank with well-mixed saltwater at 28 ppt for 4 d, depleting the oxygen levels from a saturation level of 240 to 22 ± 1 μmol L^{-1}. On the day of an experiment, a fine mesh net was used to remove all animals from the tank. The top layer of water, approximately 140 liters, was then pumped from the experimental tank into a holding tank for reoxygenation. Air stones were used to bubble the water in the holding tank for ~ 3 h in order to return the oxygen concentration to the saturated level at 21°C and atmospheric pressure. A submersible aquarium heater was simultaneously introduced into the holding tank in order to mitigate cooling from evaporation during bubbling. After reoxygenation, 2 liters of distilled water was added to the

holding tank in order to reduce the overall salinity such that the oxygenated layer would be of a lower density than the hypoxic layer. The precise water density of both tanks was measured with a density meter (Anton Paar) to confirm the stratification strength. A buoyancy frequency of the interface was used to describe the strength of the stratification based on the finite interface thickness between the two layers. This yielded $N_{\text{interface}} = 0.088 \pm 0.002\ \text{s}^{-1}$, where $N_{\text{interface}} = \sqrt{-\frac{g}{\rho_0}\frac{\Delta\rho}{\Delta z}}$ where g is gravity, ρ_0 is the reference density of 1019.165 ± 0.005 kg m^{-3}, $\Delta\rho$ is the density difference between the top and bottom layer of 0.040 ± 0.005 kg m^{-3}, and Δz is the interface thickness of 0.05 ± 0.01 m. Buoyancy frequencies were similar to values found in lake pycnoclines (Etemad-Shahidi and Imberger 2001; Hembre and Megard 2003) and higher than typical values in oceanic pycnoclines, leading to a potentially stronger suppression of vertical motion in laboratory experiments than the ocean. The oxygenated holding tank water was then pumped back into the experimental tank via a tube attached to a buoyant Styrofoam block such that the input continuously rose with the water level in order to minimize mixing with the bottom layer. This process led to a two-layer stably stratified tank with a higher density, hypoxic layer below, and a lower density, oxygenated layer on top. Mixing of the oxygenated water with the hypoxic water during the filling process reduced the upper layer oxygen levels below saturation values. A small temperature mismatch of 0.15°C was observed between the two layers, but the tank remained stably stratified in salinity and overall in density. Due to the higher diffusivity of heat vs. salt, the stable density stratification was also stable to double-diffusive fingering instabilities, and any differential diffusion of temperature only further reinforced the two-layer stratification (Radko 2013).

A computer-controlled, motorized vertical traverse (Dynamic Solutions) moving at 0.28 cm s^{-1} was used to obtain vertical profiles of the water column at multiple times during each experiment as described in the following section. A conductivity-temperature probe (Precision Measurement Engineering) measured the salinity and temperature to calculate density profiles with an accuracy of $\pm$ 0.005 kg m^{-3}. The conductivity channel had a nearly instantaneous response time, and the temperature channel had a 3 dB response time of ~ 0.007 s. The oxygen optode mounted on the same traverse simultaneously measured oxygen levels in the tank with a response time of 3 s. The oxygen optode also had a temperature sensor that automatically incorporated the temperature dependence of the oxygen measurement into the calibrated output value. The relatively slow response time of the oxygen optode led to a maximum potential shift of the oxygen profile by 0.84 cm when considering the vertical traverse speed, a negligible shift relative to other measurement uncertainty (i.e., the density probe noise). Although the slow response time may smooth centimeter-scale gradients, mixing was assessed at a full-tank scale, and thus, any local smoothing did not affect mixing estimates. Although the saturation concentration of oxygen was also dependent upon the salinity of the water, the salt-stratified water column had salinities varying by 0.15 ppt, corresponding to a variability in saturation concentration of 0.75 μmol O_2 L^{-1}, below the noise of the oxygen probe.

Controllable vertical migrations

For animal migration experiments, the strong phototactic response of the brine shrimp was utilized to produce controllable vertical migrations of aggregations of swimmers. The attraction toward the light by the brine shrimp outweighed any aversion to the hypoxic layer; therefore, animals could be drawn toward the top or bottom of the tank by corresponding lights on either side. Swimming behavior also appeared unaffected by the variable oxygen concentration. The impervious nature of the brine shrimp to variable oxygen levels has been similarly observed in situ for brine shrimp inhabiting anoxic waters (Maszczyk and Wurtsbaugh 2017).

Arrays of focused light-emitting diodes (LEDs; Outlite a100) were used to induce migration toward the light in the center of the tank, with an array situated below the clear bottom of the tank pointing upward and an array positioned above the tank pointing downward. Prior to each experiment with the animals freely swimming disaggregated in the tank, control profiles of density and oxygen were obtained every 20 min for 1 h to measure the variability due to background motions in the tank. The bottom LED array was then initially powered on to gather the animals at the bottom of the tank. To start each experiment, the bottom LED array was turned off and the top LED array was activated, inducing an upward migration of the aggregation with average swimming speeds of 0.75 ± 0.17 cm s^{-1}, determined from object tracking of individual swimmers. The column of light produced by the focused LEDs attracting the animals upward led to a concentrated aggregation of animals within the center of the tank, with local animal number densities up to 600,000 animals m^{-3}. The distribution of animal reaction times resulted in a spread of animals over the vertical extent of the tank. The first animals reached the top of the tank within 5 min and the majority of the aggregation migrated to the upper half of the tank within 10 min and proceeded to hover near the light. In order to maximize active swimming through the stratified region of the tank with a limited-size aggregation, a 10 min up–down cycling period was chosen. After 10 min, the top LED array was deactivated and the bottom LED array was turned on, returning the aggregation to the bottom of the tank. After another 10 min, the cycle was repeated, inducing another upward migration (Fig. 1). The 20 min up–down cycle was repeated six times to simulate a 120 min passage of swimmers through a stratified column, a timescale chosen to match oceanic diurnal vertical migration with a representative swimming speed of 1 cm s^{-1} and a representative aggregation with a vertical extent of 50–100 m (Sato et al. 2013), leading to a representative time of 80–170 min for an entire aggregation to pass through a fixed depth in the water column. Due to laboratory constraints on the vertical extent of the aggregation, the water column was perturbed by the same group of animals multiple times during an

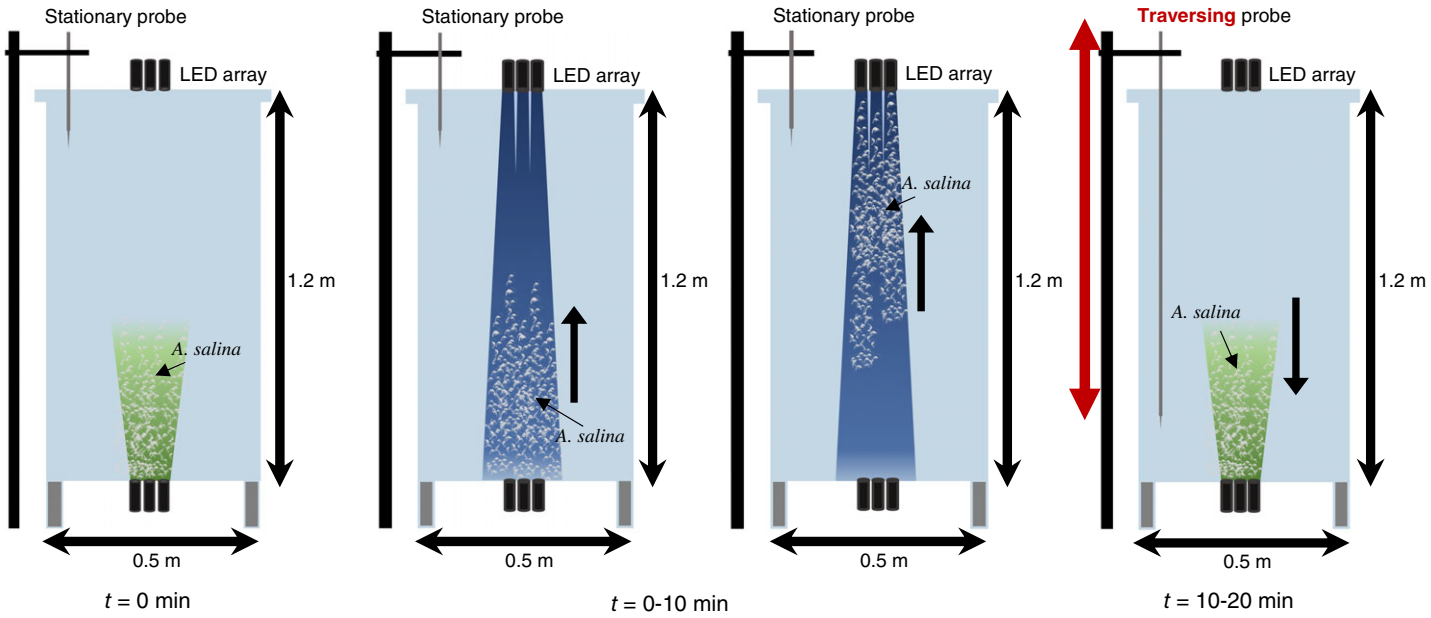

Fig. 1. Schematic of protocol during stratified mixing experiments. A 0.5 × 0.5 × 1.2-m tank with a two-layer salt and oxygen stratification was used with an array of 6 focused LEDs with blue filters introduced from the top of the tank and an array of 6 focused LEDs with green filters introduced from below for control of the migration. The 20-min cycle illustrated was repeated six times in total to give a 120-min experiment. A vertical profile of density and oxygen was obtained at 90, 120, and 140 min. Adapted from Houghton et al. (2018).

experiment as the aggregation traversed up and down. The alternation of upward and downward swimming in laboratory experiments potentially reduced cumulative effects from repeated perturbations by subsequent swimmers, in contrast to a typical oceanic vertical migration where a given parcel of water would be sequentially perturbed by multiple, distinct animals over the course of the migration. At 90 and 120 min into the experiment, oxygen and density profiles were obtained when animals were minimally active at the bottom of the tank. A repeated profile was obtained at 140 min, i.e., 20 min after the end of animal migrations, to confirm the consistency of the density profiles indicating that the tank was fully settled and horizontally homogeneous. Previous experiments by Houghton et al. (Houghton et al. 2018) demonstrated that the fluid dynamics did not change appreciably between experiments in tanks that differed in volume by a factor of five.

Data postprocessing

A single probe with a conductivity and temperature sensor was used to determine the fluid density at each height. However, the response time on the temperature sensor was slower than the conductivity sensor (McDonald 1992). Due to the dependence of salinity on the conductivity and the temperature, densities calculated in regions where temperature and salinity changed rapidly required correction (e.g., the interface between the two layers). To correct the temperature signal lag, a signal filter function developed by Fozdar et al. was used (Fozdar et al. 1985; McDonald 1992). The temperature signal was filtered following the equation:

$$T_{k,\text{filter}} = \frac{1}{1-a}(T_k - aT_{k-1})$$

where T_k is the kth value of the voltage from the temperature sensor, $a = e^{-\frac{dt}{\tau}}$, dt is the sampling interval, and τ is the sharpening time constant chosen empirically. Filtering of the temperature voltage signal introduced noise, so a low-pass filter was then applied to both the temperature and conductivity voltage signals. The two signals were then combined to calculate salinity and density. This method remediated most of the signal delay, leaving the appearance of a minor unstable density profile artifact at the interface for the sharp two-layer stratification. This artifact did not impact any subsequent analysis or conclusions.

To quantify mixing in the tank, an estimate of effective diffusivity was obtained by fitting solutions of the diffusion equation,

$$\frac{\partial C}{\partial t} = \kappa_{\text{eff}} \frac{\partial^2 C}{\partial z^2}$$

to the experimental profiles obtained, where C is the oxygen concentration and κ_{eff} is the effective diffusivity. The initial two-layer concentration profile was numerically evolved in time following the discretized form of the diffusion equation using a forward-in-time, centered-in-space explicit numerical scheme with no-flux boundary conditions at the top and bottom of the domain to obtain final density profiles for a prescribed effective diffusivity. The effective diffusivity that minimized the norm of the error between the numerically calculated and experimentally measured final oxygen concentration profile was chosen.

Signal-to-noise ratio

The experimental tank was weakly stratified relative to the resolution of instruments designed to record density stratification, even at high spatial and temporal resolution. As a result of the relatively low signal-to-noise ratio of the measured density profile, a spline fit of the data was used to quantify the density profiles. In contrast, the oxygen concentration spanned a much larger range of values relative to the probe variability of 1 μmol L^{-1}, going from strongly hypoxic (23 $\pm$ 1 μmol L^{-1}) to 60% of air saturation (144 $\pm$ 1 μmol L^{-1}). As a result, the signal-to-noise ratio for the normalized oxygen concentration was a significantly higher value of 28.0 dB relative to −1.1 dB for the normalized density.

One-dimensional hypoxic water column model

The effect of temporally intermittent migration-induced mixing relative to the continuous oxygen consumption and surface replenishment was assessed with a one-dimensional model. The evolution of an initial two-layer distribution of oxygen, with an oxygenated top layer and anoxic bottom layer, was described by the partial differential equation,

$$\frac{\partial C(z,t)}{\partial t} = \kappa_{\text{eff}}(t)\frac{\partial^2 C}{\partial z^2} - R_{\text{sink}}(z,t),$$

with the boundary conditions

$$\left.\frac{\partial C}{\partial z}\right|_{z=0} = 0$$

$$C|_{z=\text{surface}} = C_{\text{sat}}$$

where C is the oxygen concentration in μmol L^{-1}, $\kappa_{\text{eff}}(t)$ is the effective diffusivity as a function of time, $R_{\text{sink}}(z, t)$ is the depletion rate of oxygen, and C_{sat} is the saturated oxygen concentration of 250 μmol L^{-1}. A discretized form of the equation was numerically evolved in time with a no-flux condition imposed at the bottom, instantaneous oxygen equilibration of the surface with the atmosphere imposed at the surface with a constant concentration boundary condition, and oxygen levels restricted to remain non-negative.

Animal location was modulated between the upper and lower half of the water column following a diurnal cycle (i.e., every 12 h). An oxygen consumption rate, $R_{\text{sink}}(z, t)$, was used based on the experimental measurements of *A. salina* metabolism. The sink term was active only in the region occupied by animals, that is, the top half or bottom half. The effective diffusivity varied in time, defined as the diffusivity of oxygen in water for t = 0 h to t = 11 h, when animals were not migrating. For t = 11 h to t = 12 h, the effective diffusivity was increased to a value informed by the migration experiments. Following the migration, the location of the animal swarm was switched to the upper or lower half of the water column, respectively, and the 12 h cycle was repeated.

Variable animal number density

Simultaneous volumetric animal number density and two-dimensional velocity measurements were conducted in a well-mixed tank. The experimental tank was filled with 21°C salt water at 28 ppt.

Vertical migrations were induced in a manner similar to the hypoxic water column experiments, but with a single focused LED pointed vertically downward from the top of the tank that produced a column of light ~ 5 cm across that attracted the swimmers upward in a dense aggregation within the illuminated region in the center of the water column. An additional focused LED was pointed horizontally just below the height of the water surface intersecting the vertical beam to draw the swimmers to the edge of the tank after they reached the surface to reduce crowding of the swimmers and shadowing of the light. The activation of the upper LED elicited a strong reaction of the swimmers toward the light, and measurements focused on the steady migration of swimmers in the first 4 min.

After ~ 4 min, the upper LED was deactivated and the lower LED array was reactivated to return the swimmers to the bottom of the tank. Due to the slight negative animal buoyancy, animals were minimally active at the bottom of the tank leading to negligible flow disturbances during this period. The tank was then allowed to settle before restarting the migration process. Twenty-two repeated experiments were carried out over 2 d with the same batch of animals. The tank was initially filled with animals at ~ 70,000 animals m^{-3}, but actual number density within the migration was governed by endogenous animal behavior rather than total animals in the tank. Over time fewer animals partook in the migration process, either due to diminishing photo-taxis or general endurance, resulting in a range of animal number densities within the swarm among the repeated experiments.

Fluid velocity quantification

The experimental tank was seeded with 13 μm neutrally buoyant glass beads, and a 1 W, 635 nm (red) laser with a cylindrical lens (f = −9.7 mm; Newport Optics) was used to illuminate a vertical plane through the center of the aggregation. A 24 mega-pixel CMOS digital camera with a 120 mm macro lens and a 92 mm lens extender (Nikkor Nikon) was focused on the laser sheet with a field of view 1.9 cm × 3.4 cm. Video recording at 25 fps commenced immediately following the activation of the upper focused LED.

Videos were converted to frame sequences and analyzed using MATLAB (MathWorks). Pairs of subsequent frames (dT = 0.04) were used to conduct particle image velocimetry (PIV) using PIVLab (Thielicke and Stamhuis 2014) to calculate vertical and horizontal velocities in the laser-illuminated two-dimensional slice through the center of the aggregation. Images were interrogated using a multipass method with two iterations and a decreasing window size from 64 × 64 pixels to 32 × 32 pixels and a 50% overlap. Prior to PIV processing, animals within the field of view were masked, with the identical mask applied to both frames interrogated for each velocity calculation.

Animal number density quantification

The column of light produced by the focused LED used to induce the migrations illuminated animals within a known volume to allow approximation of the animal number density in the field of view over time. Animal count in each video frame was calculated via image segmentation using the watershed transform (Gonzalez and Woods 2002) to optimally differentiate between overlapping animals. As only animals within the light column were visible to the camera, the volume in which the counted animals were contained was calculated as the camera field of view (1.9 cm × 3.4 cm) by the width of the LED beam at the height of the camera (5.0 cm). This method provided an estimate of instantaneous animal number density with the assumption of homogeneous animal spacing within the illuminated volume. Both the heterogeneous animal spacing and the animal density decay in the out-of-plane direction following the horizontal decay of the light column were not accounted for in this approximation.

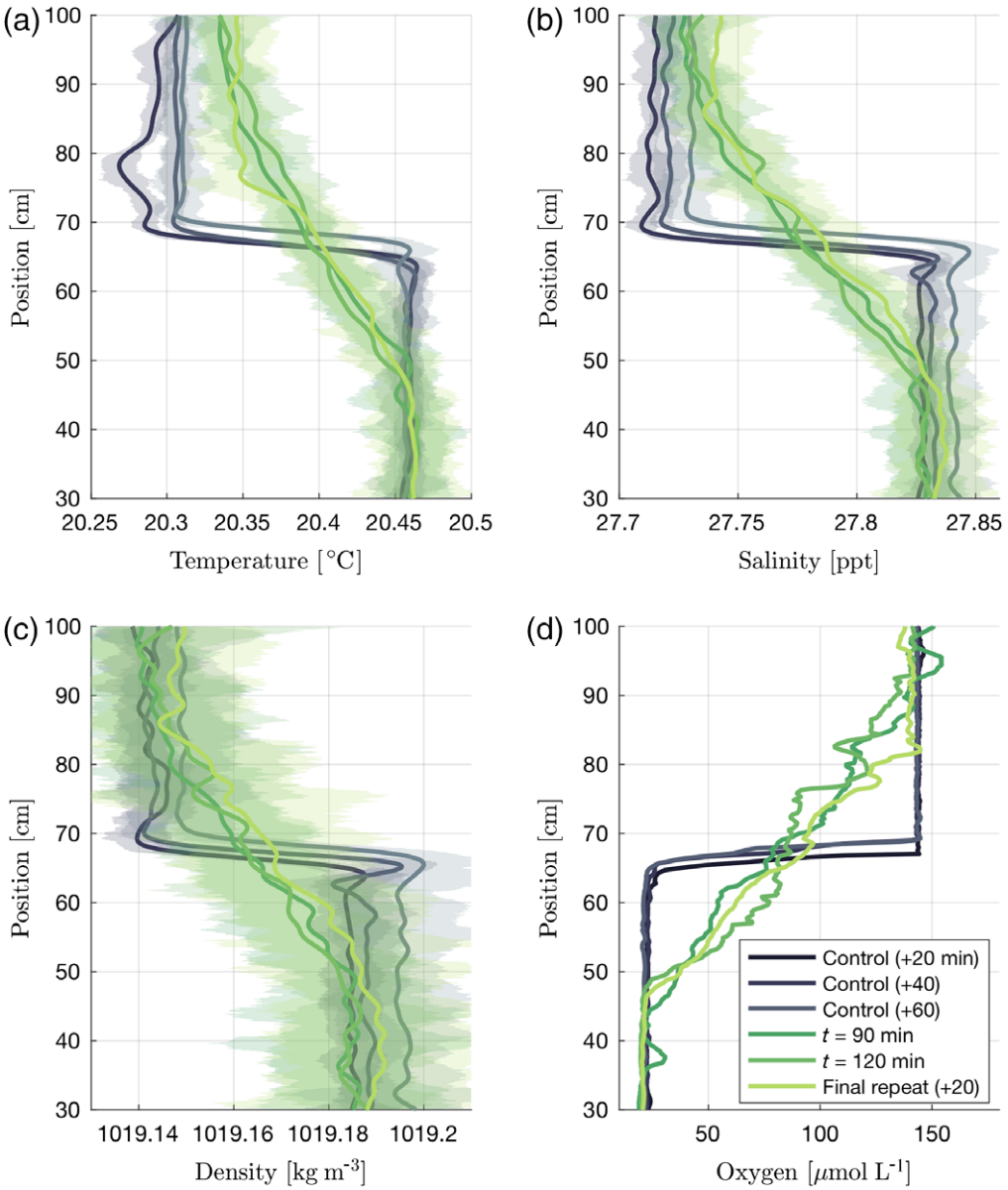

Fig. 2. Profiles of temperature (**a**), salinity (**b**), density (**c**), and oxygen (**d**) during migration experiments. Black lines correspond to control profiles obtained prior to animal migrations. Green lines correspond to profiles during and after repeated animal migrations. Spline fits were used to display the temperature, salinity, and density signals separate from the noise of the probes, with the average noise shown in the shaded envelopes. All profiles indicated significant mixing of the stratified scalars.

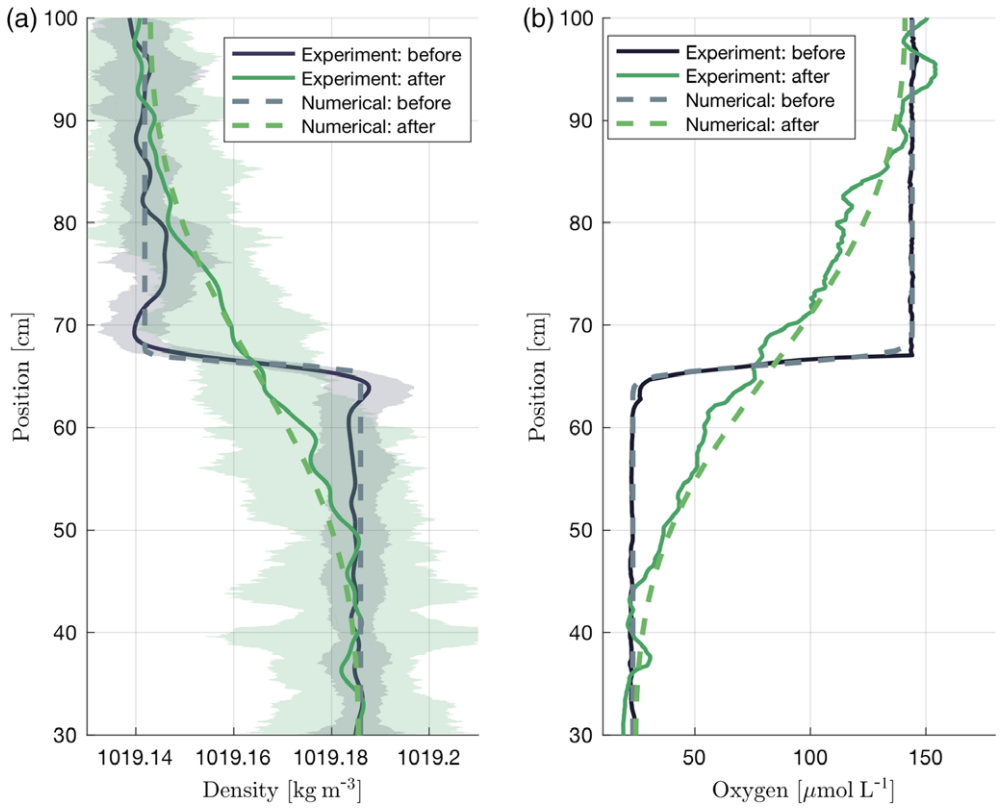

Fig. 3. An effective diffusivity of κ_{eff} = 0.006 cm^2 s^{-1} minimized the norm of the error between the experimentally measured and numerically calculated profiles for density (**a**) and oxygen (**b**) with the numerically calculated final profiles shown overlaid on the experimental profiles. Both oxygen and density evolved similarly within the noise of the probes.

Results

Hypoxia experiment measurements

Figure 2 illustrates the evolution of the temperature, salinity, density, and oxygen over the course of the migration experiments. Notable mixing of the water column occurred, similar to previous findings (Houghton et al. 2018), and both salt and oxygen concentrations evolved similarly. Fitting the diffusion equation to experimental profiles for density and oxygen yielded an effective diffusivity of 0.006 $\pm$ 0.001 cm^2 s^{-1} (Fig. 3), consistent with previous results by Houghton et al. (2018).

Both scalars yielded equivalent effective diffusivities, indicating that oxygen, with a molecular diffusivity in water similar to salt (D_{O_2} = 2.0 $\times$ 10^{-5} cm^2 s^{-1}; Ferrell and Himmelblau 1967), evolved in time following the density profile. Depletion of oxygen below the original lowest level in the hypoxic layer was not observed during the 2 h migration experiment. Moreover, total dissolved oxygen in the tank remained constant within measurement resolution, with cumulative oxygen levels fluctuating $\pm$ 3% from the mean value with no clear decreasing trend in time over the 2 h experiment.

The oxygen consumption rate determined from the control experiment indicated notably slower losses, with an oxygen depletion rate of ~ 1.8 μmol L^{-1} h^{-1} vs. concentration changes up to 43 μmol L^{-1} h^{-1} during the migration experiment (Fig. 2d). The 48 h evolution of the oxygen concentration was slightly nonlinear, with a lower depletion rate at lower dissolved oxygen concentrations. However, the lower oxygen concentration occurred simultaneously with diminishing animal health and increased animal mortality, thereby affecting cumulative oxygen consumption. Altogether, oxygen consumption occurred significantly more slowly than mixing, making biogenic mixing the primary driver of changes in oxygen distribution in the tank during migration experiments.

Numerical model

The one-dimensional model simulated the evolution of the oxygen profile over a multiday timescale. Figure 4 illustrates the notable difference with the inclusion of biogenic mixing, despite the enhanced mixing occurring only intermittently. While simplifying a variety of complex physical and chemical dynamics, such as the role of horizontal heterogeneity, the model illustrated the capacity for the enhanced biogenic mixing to alter the exchange of oxygen between layers with a notable impact relative to metabolic consumption, even over several days. This manifested as an increased flux of oxygen into the lower layer, potentially delaying the onset of hypoxia and increasing the habitability of the intermediate region.

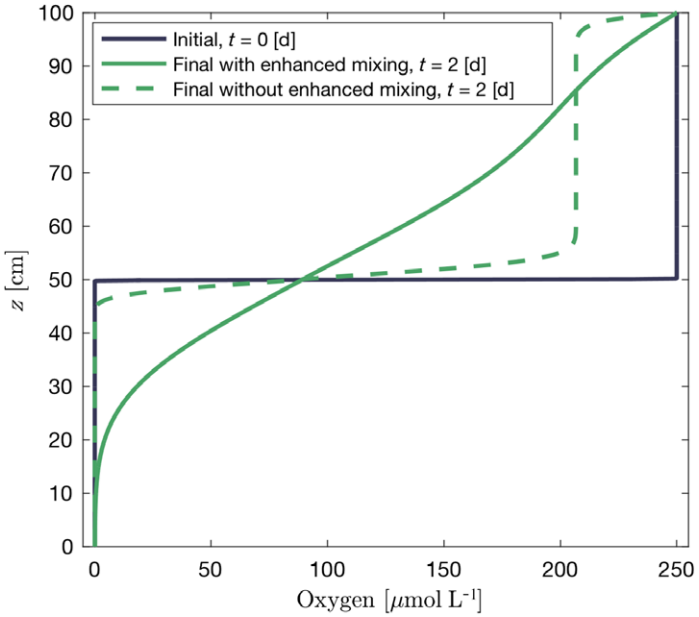

Fig. 4. Model results for oxygen concentration profiles after 2 d of oxygen depletion, surface replenishment, and diurnal periods of enhanced mixing (solid green line). Relative to the case without enhanced mixing during migrations (dashed green line), notably higher oxygen concentrations persisted in the lower layer.

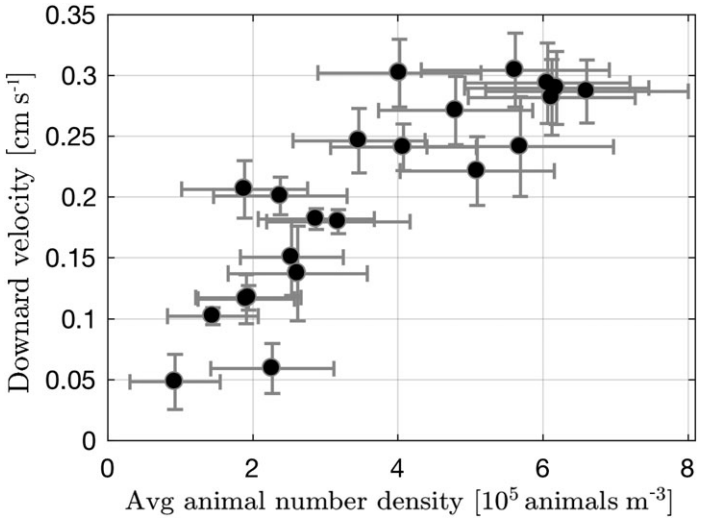

Fig. 5. The spatially averaged downward fluid velocity as a function of animal number density in the developed migration. Error bars represent the standard deviation of the animal count (horizontal) and fluid velocity (vertical). The standard deviation of the animal count is due to animal density variability during the asymptotic period as well as large noise in the counting algorithm.

Animal number density dependency

In all 22 migrations measuring fluid transport as a function of animal number density, similar dynamics evolved. Within 2 min following activation of the upper LED, animal number density in the field of view reached an approximately constant level and a spatially coherent downward flow developed. Due to variability in animal participation in the migration between repeated trials, the asymptotic animal number density varied between each trial, allowing comparison of fluid transport. Migrations with a higher asymptotic animal number density resulted in a larger spatially averaged downward velocity (Fig. 5). Within the animal number density range tested (~ 100,000–600,000 animals m^{-3}), the downward coherent flow strength increased roughly linearly. Comparison between unstratified experiments and stratified experiments indicated that the steady-state induced vertical velocities were qualitatively similar in both cases and stratification did not arrest the vertical fluid transport from extending throughout the entire aggregation.

Discussion

The enhancement of mixing of all stratified scalars observed in laboratory experiments indicates that the passage of swimming zooplankton at sufficiently high concentration has the potential to significantly alter the biogeochemical structure of the water column. As described in previous work by Houghton et al. (2018), large-scale transport and eddy motion within the stable density stratification due to the collective animal propulsion increases the surface area and concentration gradients between the high and low-density fluid, enhancing diffusivity and leading to irreversible mixing of the salt and oxygen concentration. In terms of Peclét number,

$$Pe = \frac{ul}{D}$$

where u is the representative fluid velocity, l is the representative length-scale of the aggregation, and D is the diffusivity of oxygen, these experiments occurred at ~ 7×10^5, indicating the dominance of advective over diffusive transport. Similarly, in terms of Damköhler number,

$$Da = \frac{dO_{2,\,\mathrm{metabolic}}}{dO_{2,\,\mathrm{mixing}}}$$

where $dO_{2,\,\mathrm{metabolic}}$ is the rate of change of oxygen due to metabolic consumption and $dO_{2,\,\mathrm{mixing}}$ is the mass transport rate of oxygen due to mixing, values were approximately 0.04, indicating the dominance of mixing in determining the oxygen distribution.

Fluid velocity within the aggregation is roughly linearly dependent upon animal number density. Conceptually, the enhanced mixing characterized by an effective diffusivity, κ_{eff}, scales as the product of the characteristic velocity of the flow and the characteristic length scale. As the length scale is set by the vertical extent of the aggregation (Houghton et al. 2018), the linear scaling of vertical velocity with animal number density (Fig. 5) suggests that κ_{eff} also scales linearly. For extension to zooplankton of variable size, the animal volume fraction may be more representative of an equivalent regime. The

range of animal number densities and the corresponding volume fractions in laboratory experiments are on the same order of magnitude as a number of in situ observations (O'Brien 1988; Hembre and Megard 2003), indicating the potential for dynamics similar to laboratory experiments to occur in the field with corresponding impacts to mixing of density and oxygen distributions.

By mixing oxygen downward into an oxygen-depleted zone, potential feedbacks among animal presence, gas and nutrient exchange, and habitability arise. The disparity between the timescales for oxygen consumption and oxygen mixing by the swimming zooplankton indicates that during periods of active swimming—either vertical migration or hovering—zooplankton can potentially alleviate hypoxia due to their swimming motions. In terms of the diurnal cycles observed in lakes and oceans, where zooplankton descend into hypoxic layers during the day, this behavior could result in unique feedbacks for habitability beneath the pycnocline. Although other biological activity may more rapidly deplete oxygen, migrating zooplankton may serve as an alleviating factor. Field observations of large-scale biologically induced flows remain sparse (Sommer et al. 2017; Tarling and Thorpe 2017), therefore novel field investigations will be critical in understanding the extent of this laboratory-observed phenomenon.

While the effective diffusivity is characterized for active migration periods, persistent large-scale flow was also observed within hovering swarms and has been similarly documented via acoustics within krill swarms in the field (Tarling and Thorpe 2017). Due to slight negative animal buoyancy, similar to most marine zooplankton (Pond 2012), downward thrust must be generated in order to maintain vertical position while hovering. For many zooplankton species, this thrust is produced via the rearward propulsion of fluid (Catton et al. 2011; Murphy et al. 2013; Wilhelmus and Dabiri 2014), leading to transport within the aggregation. With large-scale vertical fluid transport occurring not only during diurnal migration periods but also during prolonged intermediate periods when animals hover at the surface or at depth, even greater biogeochemical impacts could be expected. As zooplankton often take refuge just below the pycnocline or just within a hypoxic region in daytime (Vanderploeg et al. 2009; Bianchi et al. 2013) significant vertical transport of water with high variability in density, nutrients, and oxygen could occur throughout an entire day, rather than only during diurnal migration periods. This continuous vertical transport and mixing could have significant implications for the habitability of that layer, potentially sustaining the animal presence with unique behavioral feedbacks.

Within aggregations of swimmers, the hydrodynamic interactions between the swimming organisms will be governed by the Reynolds number of the flow induced by individual swimmers, as that will determine the balance between the persistence of the rearward jet due to inertia and its viscous diffusion. The Reynolds number for these experiments with the brine shrimp *A. salina* is approximately 50. Furthermore, the competition between persistence of the rearward vertical jet in stratified flow and its suppression by the stable stratification can be quantified by a Froude number based on vertical velocity and the density contrast, which in these laboratory experiments is ~ 0.02. Flow visualization indicated strong recirculation of displaced fluid outside the aggregation (Houghton et al. 2018), indicative of the importance of the background stratification in dynamics. A match of these two parameters can enable comparison with future lab experiments or observations under naturally occurring conditions.

Laboratory experiments illustrated the correlation between mixing of density and of oxygen, despite potentially more complex source and sink dynamics of the latter. Interestingly, the signal-to-noise ratio for oxygen was significantly higher than for density. In light of ongoing efforts to address the significance of biogenic mixing in situ (Kunze 2006; Gregg and Horne 2009; Katija and Dabiri 2009; Rousseau et al. 2010), variables with high signal-to-noise ratios could provide an effective means for quantifying impacts to the water column. Although sources and sinks from other variables are also potentially critical, these laboratory experiments demonstrate that the predominant driver of oxygen concentrations over these timescales arises from biogenic mixing rather than metabolic consumption. Given similar timescales of investigation in the field (i.e., minutes to hours during a migration event), detection of altered oxygen distributions could be a powerful indicator of the importance of biogenic mixing due to its relatively strong signal.

Altogether, the laboratory experiments and an analytical model indicate the potential relevance of biologically induced mixing of oxygen, leading to the potential for an active role of animals in relieving hypoxia and determining the surrounding habitability for themselves and other species.

A recent survey of research on biologically-generated mixing concluded that the effect of swimming organisms on mixing is small in the ocean (Kunze 2019). This conclusion is based primarily on a limited set of microstructure measurements collected in the vicinity of animal aggregations in the ocean, as well as order-of-magnitude scaling arguments. The present results challenge those scaling arguments, showing that solutes and dissolved gases can indeed be mixed to a significant degree and over large length scales during vertical migration of small organisms. Future field studies should endeavor to complement microstructure measurements with more direct observations of the full velocity field induced by swimming aggregations and the corresponding impact, if any, on background gradients in the water column. Such measurements present the best opportunity for definitive answers regarding the potential role of biologically generated mixing in the ocean. Altogether, further field investigation will be essential to achieve a more comprehensive understanding of the complex dynamics and feedbacks between migrating zooplankton and their environment, and oxygen may be an especially useful target for examination.

References

Bianchi, D., E. D. Galbraith, D. A. Carozza, K. A S Mislan, and C. A. Stock. 2013. Intensification of open-ocean oxygen depletion by vertically migrating animals. Nat. Geosci. **6**: 545–548. doi:10.1038/ngeo1837

Butterfield, N. J. 2018. Oxygen, animals and aquatic Bioturbation: An updated account. Geobiology **16**: 3–16. doi:10.1111/gbi.12267

Catton, K. B., D. R. Webster, S. Kawaguchi, and J. Yen. 2011. The hydrodynamic disturbances of two species of krill: Implications for aggregation structure. J. Exp. Biol. **214**: 1845–1856. doi:10.1242/jeb.050997

Dewar, W. K., R. J. Bingham, R. L. Iverson, D. P. Nowacek, L. C. St. Laurent, and P. H. Wiebe. 2006. Does the marine biosphere mix the ocean? J. Mar. Res. **64**: 541–561. doi:10.1357/002224006778715720

Diaz, R. J. 2001. Overview of hypoxia around the world. J. Environ. Qual. **30**: 275. doi:10.2134/jeq2001.302275x

Diaz, R. J., and R. Rosenberg. 2008. Spreading consequences dead zones and consequences for marine ecosystems. Science **321**: 926–929. doi:10.1126/science.1156401

Etemad-Shahidi, A., and J. Imberger. 2001. Anatomy of turbulence in thermally Stratified Lakes. Limnol. Oceanogr. **46**: 1158–1170. doi:10.4319/lo.2001.46.5.1158

Ferrell, R. T., and D. M. Himmelblau. 1967. Diffusion coefficients of nitrogen and oxygen in water. J. Chem. Eng. Data **12**: 111–115. doi:10.1021/je60032a036

Fozdar, F. M., G. J. Parker, and J. Imberger. 1985. Matching temperature and conductivity sensor responce characteristics. J. Phys. Oceanogr. **15**: 1557–1569. doi:10.1175/1520-0485(1985)015<1557:MTACSR>2.0.CO;2

Gonzalez, R., and R. Woods. 2002. Digital image processing. Prentice Hall.

Gregg, M. C., and J. K. Horne. 2009. Turbulence, acoustic backscatter, and pelagic nekton in Monterey Bay. J. Phys. Oceanogr. **39**: 1097–1114. doi:10.1175/2008JPO4033.1

Hamner, W. M., P. P. Hamner, S. W. Strand, and R. W. Gilmer. 1983. Behavior of Antarctic krill, *Euphausia superba*: Chemoreception, feeding, schooling, and molting. Science **220**: 433–435. doi:10.1126/science.220.4595.433

Hembre, L. K., and R. O. Megard. 2003. Seasonal and Diel patchiness of a daphnia population: An acoustic analysis. Limnol. Oceanogr. **48**: 2221–2233. doi:10.4319/lo.2003.48.6.2221

Houghton, I. A., J. R. Koseff, S. G. Monismith, and J. O. Dabiri. 2018. Vertically migrating swimmers generate aggregation-scale eddies in a stratified column. Nature **556**: 497–500. doi:10.1038/s41586-018-0044-z

Huntley, M. E., and M. Zhou. 2004. Influence of animals on turbulence in the sea. Mar. Ecol. Prog. Ser. **273**: 65–79. doi:10.3354/meps273065

Katija, Kakani, and John O Dabiri. 2009. A viscosity-enhanced mechanism for Biogenic Ocean mixing. Nature **460**: 624–626. doi:10.1038/nature08207, 460, 7255.

Kunze, E. 2006. Observations of biologically generated turbulence in a coastal inlet. Science **313**: 1768–1770. doi:10.1126/science.1129378

Kunze, E. 2019. Biologically generated mixing in the ocean. Ann. Rev. Mar. Sci. **11**. Annual Reviews: 215–226. doi:10.1146/annurev-marine-010318-095047

Longhurst, A. R., and W. Glen Harrison. 1988. Vertical nitrogen flux from the oceanic photic zone by Diel migrant zooplankton and nekton. Deep-Sea Res. Part A. Oceanogr. Res. Pap. **35**: 881–889. doi:10.1016/0198-0149(88)90065-9

Manno, C., G. Stowasser, P. Enderlein, S. Fielding, and G. A. Tarling. 2015. The contribution of zooplankton faecal pellets to deep-carbon transport in the Scotia Sea (Southern Ocean). Biogeosciences **12**: 1955–1965. doi:10.5194/bg-12-1955-2015

Maszczyk, P., and W. A. Wurtsbaugh. 2017. Brine shrimp grazing and fecal production increase sedimentation to the deep brine layer (Monimolimnion) of Great Salt Lake, Utah. Hydrobiologia **802**: 7–22. doi:10.1007/s10750-017-3235-y

McDonald, Ellen. 1992. The dynamics and structure of lateral intrusions in a continuously stratified heat/salt system. Available from http://sul-sfx.stanford.edu/sfxlcl41?url_ver=Z39.88-2004&rft_val_fmt=info%3Aofi%2Ffmt%3Akev%3Amtx%3Adissertation&genre=dissertations %26 theses&sid=ProQ%3ADissertations %26 Theses %40 Stanford University&atitle=&title=The dynamics and structure of lateral

Murphy, D. W., D. R. Webster, and J. Yen. 2013. The hydrodynamics of hovering in Antarctic krill. Limnol. Oceanogr.: Fluids Environ. **3**: 240–255. doi:10.1215/21573689-2401713

Noss, C., and A. Lorke. 2014. Direct observation of biomixing by vertically migrating zooplankton. Limnol. Oceanogr. **59**: 724–732. doi:10.4319/lo.2014.59.3.0724

O'Brien, D. 1988. Surface schooling behaviour of the coastal krill *Nyctiphanes Australis* (Crustacea: Euphausiacea) off Tasmania, Australia. Mar. Ecol. Prog. Ser. **42**: 219–233. doi:10.3354/meps042219

Omori, M, and W M Hamner. 1982. Patchy distribution of zooplankton: Behavior, population assessment and sampling problems. Mar. Biol. **72**. Springer-Verlag: 193–200. doi:10.1007/bf00396920

Osborn, T. R. 1980. Estimates of the local rate of vertical diffusion from dissipation measurements. J. Phys. Oceanogr. **10**: 83–89. doi:10.1175/1520-0485(1980)010%3C0083:eotlro%3E2.0.co;2

Pond, D. W. 2012. The physical properties of lipids and their role in controlling the distribution of zooplankton in the oceans. J. Plankton Res. **34**: 443–453. doi:10.1093/plankt/fbs027

Radko, T. 2013. Double-diffusive convection. Cambridge Univ. Press, Available from http://www.worldcat.org/isbn/9780521880749.

Ringelberg, J. 2009. Diel vertical migration of zooplankton in lakes and oceans: Causal explanations and Adaptative significances. Springer.

Ringelberg, J. 2014. Diel vertical migration of zooplankton in lakes and oceans. Springer. doi:10.1007/s13398-014-0173-7.2

Rousseau, S., E. Kunze, R. Dewey, K. Bartlett, and J. Dower. 2010. On turbulence production by swimming marine organisms in the open ocean and coastal waters. J. Phys. Oceanogr. **40**: 2107–2121. doi:10.1175/2010jpo4415.1

Sato, M., J. F. Dower, E. Kunze, and R. Dewey. 2013. Second-order seasonal variability in diel vertical migration timing of Euphausiids in a coastal inlet. Mar. Ecol. Prog. Ser. **480**: 39–56. doi:10.3354/meps10215

Simoncelli, S., S. J. Thackeray, and D. J. Wain. 2018. On biogenic turbulence production and mixing from vertically migrating zooplankton in lakes. Aquat. Sci. **80**: 35. doi: 10.1007/s00027-018-0586-z

Sommer, T., F. Danza, J. Berg, A. Sengupta, G. Constantinescu, T. Tokyay, H. Bürgmann, Y. Dressler, O. Sepúlveda Steiner, C. J. Schubert, M. Tonolla, and A. Wüest. 2017. Bacteria-induced mixing in natural waters. Geophys. Res. Lett. **44**: 9424–9432. doi:10.1002/2017GL074868

Tarling, G. A., and S. E. Thorpe. 2017. Oceanic swarms of Antarctic krill perform satiation sinking. Proc. Biol. Sci. **284**: 20172015. doi:10.1098/rspb.2017.2015

Thielicke, W., and E. J. Stamhuis. 2014. PIVlab—towards user-friendly, affordable and accurate digital particle image velocimetry in MATLAB. J. Open Res. Softw. **2**: e30. doi: 10.5334/jors.bl

Vanderploeg, H. A., S. A. Ludsin, J. F. Cavaletto, T. O. Höök, S. A. Pothoven, S. B. Brandt, J. R. Liebig, and G. A. Lang. 2009. Hypoxic zones as habitat for zooplankton in Lake Erie: Refuges from predation or exclusion zones? J. Exp. Mar. Biol. Ecol. **381**: S108–S120. doi:10.1016/j.jembe.2009.07.015

Visser, A. W. 2007. Biomixing of the oceans? Science **316**: 838–839. doi:10.1126/science.1141272

Wang, S., and A. M. Ardekani. 2015. Biogenic mixing induced by intermediate Reynolds number swimming in stratified fluids. Sci. Rep. **5**: 17448. doi:10.1038/srep17448

Wilhelmus, M. M., and J. O. Dabiri. 2014. Observations of large-scale fluid transport by laser-guided plankton aggregations. Phys. Fluids **26**: 1–12. doi:10.1063/1.4895655

Zhang, X., and H. G. Dam. 1997. Downward export of carbon by Diel migrant Mesozooplankton in the central equatorial Pacific. Deep-Sea Res. II Top. Stud. Oceanogr. **44**: 2191–2202. doi:10.1016/s0967-0645(97)00060-x

Acknowledgments

We thank M. M. Wilhelmus for the original development of laboratory-controlled migrations and for advice on development of the current facility and D. Koweek for helpful advice on design of oxygen experiments. We also gratefully acknowledge funding from the U.S. National Science Foundation (grant 1510607).

Author Contribution Statement

I.A.H. and J.O.D. designed the experiments, interpreted the data, and drafted the manuscript. I.A.H. conducted all experiments.

Conflict of Interest

None declared

Submitted 28 September 2018
Revised 18 December 2018
Accepted 20 March 2019

Associate editor: Leon Boegman